BIOCHEMISTRY
including biophysical chemistry & molecular biology

Article

pubs.acs.org/biochemistry

The Natural Product Dihydrotanshinone I Provides a Prototype for Uncharged Inhibitors That Bind Specifically to the Acetylcholinesterase Peripheral Site with Nanomolar Affinity

Veena Beri,[†] Scott A. Wildman,[‡] Kazuro Shiomi,[§] Ziyad F. Al-Rashid,[∥] Jonah Cheung,[⊥] and Terrone L. Rosenberry*,[†]

[†]Departments of Neuroscience and Pharmacology, Mayo Clinic College of Medicine, Jacksonville, Florida 32224, United States
[‡]Department of Biochemistry and Molecular Biophysics, Washington University, St. Louis, Missouri 63110, United States
[§]Kitasato Institute for Life Sciences, Kitasato University, Tokyo 108-8641, Japan
[∥]Alchemical Research, Bethlehem, Pennsylvania 18018, United States
[⊥]New York Structural Biology Center, New York, New York 10027, United States

ABSTRACT: Cholinergic synaptic transmission often requires extremely rapid hydrolysis of acetylcholine by acetylcholinesterase (AChE). AChE is inactivated by organophosphates (OPs) in chemical warfare nerve agents. The resulting accumulation of acetylcholine disrupts cholinergic synaptic transmission and can lead to death. A potential long-term strategy for preventing AChE inactivation by OPs is based on evidence that OPs must pass through a peripheral site or P-site near the mouth of the AChE active site gorge before reacting with a catalytic serine in an acylation site or A-site at the base of the gorge. An ultimate goal of this strategy is to design compounds that bind tightly at or near the P-site and exclude OPs from the active site while interfering minimally with the passage of acetylcholine. However, to target the AChE P-site with ligands and potential drugs that selectively restrict access, much more information must be gathered about the structure−activity relationships of ligands that bind specifically to the P-site. We apply here an inhibitor competition assay that can correctly determine whether an AChE inhibitor binds to the P-site, the A-site, or both sites. We have used this assay to examine three uncharged, natural product inhibitors of AChE, including aflatoxin B1, dihydrotanshinone I, and territrem B. The first two of these inhibitors are predicted by the competition assay to bind selectively to the P-site, while territrem B is predicted to span both the P- and A-sites. These predictions have recently been confirmed by X-ray crystallography. Dihydrotanshinone I, with an observed binding constant (K_I) of 750 nM, provides a good lead compound for the development of high-affinity, uncharged inhibitors with specificity for the P-site.

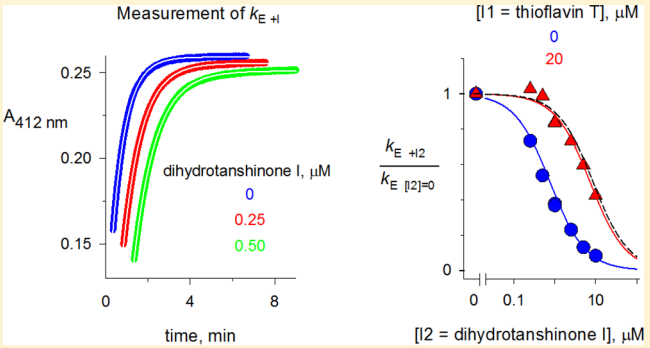

Acetylcholinesterase (EC 3.1.1.7) is one of the most important enzymes of the vertebrate nervous system. It hydrolyzes the neurotransmitter acetylcholine into choline and acetate at one of the highest known enzymatic rates[1] and is involved in the transmission of signals at synapses between nerves and between nerves and muscles.[2] Application of drugs at concentrations that partially inhibit AChE can increase the levels of acetylcholine and potentiate its physiological effects. This is the rationale for the therapeutic use of AChE inhibitors that penetrate the blood−brain barrier for symptomatic treatment of several neurological disorders, including Alzheimer's disease, in which cholinergic neurons are lost and endogenous levels of acetylcholine are decreased.[3] AChE inhibitors largely selective for insect AChEs also have been developed as pesticides. However, some inhibitors like the organophosphates (OPs) in chemical warfare nerve agents can completely block AChE activity[4] by covalently reacting with the S203 residue in the AChE active site. This results in accumulation of acetylcholine in cholinergic synapses and leads to failure of cholinergic synaptic transmission, deterioration of neuromuscular junctions, flaccid muscle paralysis, seizures in the central nervous system, and, ultimately, death.

Better insight into the interaction of inhibitors with AChE may provide new strategies for protecting against OP inactivation of AChE. Kinetic and thermodynamic studies have revealed that inhibitors can interact with either or both of two binding sites in AChE,[5−8] and X-ray crystallography has provided information about the location of these sites.[9−12] A narrow active site gorge some 20 Å deep penetrates nearly to the center of the ∼65 kDa catalytic subunits (Figure 1A). Near the base of this gorge, H447, E334, and S203[a] participate in a triad that catalyzes the transient acylation and deacylation of

Received: August 1, 2013
Revised: September 16, 2013
Published: September 17, 2013

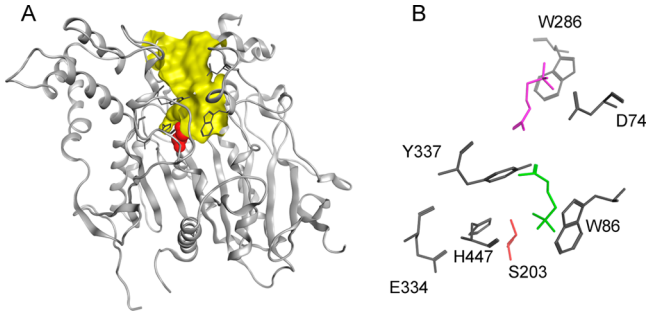

Figure 1. (A) Cross section of AChE with the active site gorge colored yellow and S203 colored red. (B) Additional key residues in the active site gorge are colored gray with their residue number.[a] The orientation is identical to that of panel A. Acetylcholine molecules observed in the crystal structure of the S203A mutant[14] are inserted into the P-site (pink) and the A-site (green). This mutation does not alter the structure of native AChE but abolishes all catalytic activity, allowing acetylcholine ligands and their binding sites in AChE to be preserved.

S203 during each substrate turnover. Two molecules of substrate can be detected in the active site gorge when acetylcholine or acetylthiocholine is diffused into crystals of *Tc*AChE[13] or the inactive S203A mutant of mouse AChE.[14] One substrate molecule in contact with W286, Y124, and D74 in mouse AChE indicates the peripheral site or P-site, and the second molecule interacting with W86 near the catalytic triad specifies the acylation site or A-site. The mobile side chain of Y337 is at the boundary between the two sites (Figure 1B). The P-site specifically binds certain ligands like the fluorescent probes propidium[6] and thioflavin T,[7] and it is included in the extensive AChE surface area bound by the neurotoxin fasciculin.[15,16] The P-site thus far has been shown to contribute to catalytic efficiency by ensuring that most substrate molecules that collide with and transiently bind to the P-site proceed to the A-site[17−19] and, with certain bound cationic substrates, by providing a modest allosteric activation of the acylation step.[20]

One antidote to OP toxicity involves cationic oximes that act as strong nucleophiles to remove an OP from S203 in the A-site and restore AChE activity[21] in individuals who have already been exposed to OPs. We are exploring a new strategy for developing drugs that prevent AChE inactivation by OPs while still maintaining adequate hydrolysis of acetylcholine by AChE. This strategy is suggested by data showing that bound P-site ligands block the entry and exit rates of ligands specific for the A-site by factors of up to 400.[18,22] We seek compounds that bind very tightly at or near the P-site and are able to selectively exclude OPs from the A-site while showing minimal interference with the entry of acetylcholine. To pursue this strategy, we need to learn more about the structure−activity relationships of ligands that bind selectively to the P-site. Unfortunately, this area of study has largely been ignored. We have applied virtual screening to identify compounds that bind specifically to the P-site, and one compound with such specificity but rather low affinity was identified.[23] Higher-affinity ligands specific for the P-site are needed as lead compounds, which provide templates for modification to achieve even greater efficacy and specificity. Such compounds will allow us not only to refine and expand virtual screening tools but also to test experimentally the effects of synthetic modifications.

To identify better candidates for a lead P-site inhibitor, we turned to several natural products. During millions of years of coexistence with animals, plants and fungi have developed a variety of mechanisms of defense. One important defense mechanism is the production of chemicals that adversely affect important physiological functions in animals. These natural products offer amazing structural diversity and distinct modes of action that have led to a resurgence of interest in this field over the past three decades. Molecular sites of action for many of these compounds are being identified, although it is important to remember that a compound may have additional, unidentified molecular sites of action that are responsible for its primary physiological effects.[24] Natural products have been reported to inhibit AChE activity and possibly bind selectively to the P-site. We are particularly interested in uncharged P-site inhibitors that may be less likely to interfere with the entry trajectory of cationic acetylcholine. Aflatoxin B1 (Figure 2) is a

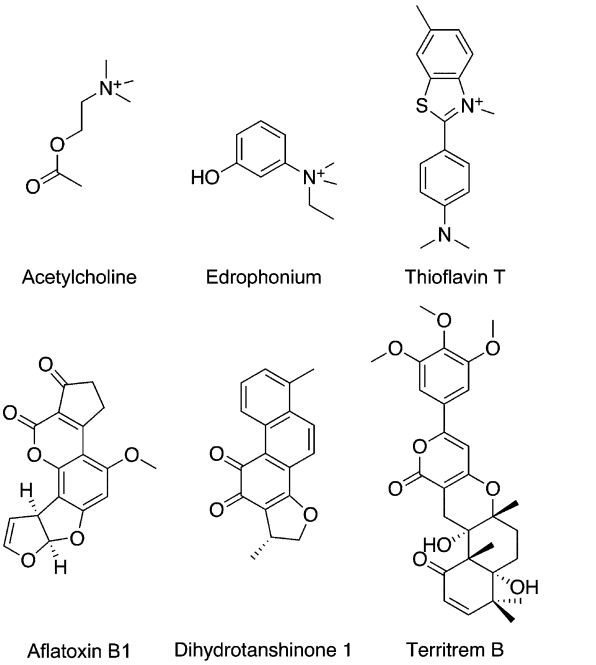

Figure 2. Molecular structures of acetylcholine and AChE inhibitors. The structures are oriented so that the moieties directed toward the mouth of the AChE active site gorge are at the top of each structure and those nearest the catalytic triad in the A-site are at the bottom. The orientation for acetylcholine is the one found at the P-site.

fungal metabolite produced by species of *Aspergillus* that can contaminate human and animal food stocks.[25,26] Its carcinogenicity,[27] extreme toxicity,[28] and relatively low affinity for mammalian AChE[29,30] make it unattractive as a potential lead compound in this study, but it is included here because it is uncharged and the first natural product inhibitor of AChE shown to bind exclusively to the P-site by X-ray crystallography.[31] Dihydrotanshinone I (Figure 2) is a diterpenoid that was first isolated from the roots of *Salvia miltiorrhiza*,[32] an angiosperm that belongs to the family Lamiaceae, and it has been widely used as a Chinese folk medicine for the treatment of cardiovascular diseases.[33] While it inhibits the activities of cyclooxygenase-2 and inducible NO synthase[34] and of diacylglycerol acyltransferase,[35] dihydrotanshinone I showed a relatively high affinity as an inhibitor of human AChE (K_I of 0.6 μM). Binding was suggested to involve aromatic residues in the P- or A-site,[36,37] and one molecular docking simulation indicated binding to the A-site.[36,37] Territrem B (Figure 2), a

dx.doi.org/10.1021/bi401043w | *Biochemistry* 2013, 52, 7486−7499

fungal meroterpenoid isolated from *Aspergillus terreus*, induces tremor and convulsions in mice on intraperitoneal administration.[38] It is a potent inhibitor of AChE with high selectivity relative to butyrylcholinesterase, and its binding to electric eel AChE was reported to be irreversible.[39] Molecular modeling indicated extensive overlap of territrem B with the P-site and less overlap with the A-site.[39] Molecular docking studies of the closely related (+)-arisugacin A meroterpenoid suggested alternative binding modes, either exclusively with the P-site or spanning the P- and A-sites.[40] Here we make use of an inhibitor competition assay that can distinguish whether an inhibitor is bound to the A-site or the P-site. The reliability of this assay has been confirmed with inhibitor standards whose sites of binding have already been identified by X-ray crystallography.[7,23,41,42] We have employed this assay to resolve the overlap of bound dihydrotanshinone I and territrem B with the P- and A-sites of AChE.

EXPERIMENTAL PROCEDURES

Materials. Recombinant human AChE was expressed as a secreted, disulfide-linked dimer in *Drosophila* S2 cells and purified as outlined previously.[43] Edrophonium chloride, 5,5′-dithiobis(2-nitrobenzoic acid) (DTNB), acetylthiocholine iodide (AcSCh), aflatoxin B1, and bovine serum albumin (BSA), Fraction V (approximately 99%), were obtained from Sigma-Aldrich Chemical Co. (St. Louis, MO). Thioflavin T (Sigma-Aldrich) was recrystallized from water, and concentrations were assigned by the absorbance at 412 nm with an ε_{412} of 36000 M^{-1} cm^{-1}. Aflatoxin B1 (Sigma-Aldrich) concentrations were determined from an ε_{362} of 21800 M^{-1} cm^{-1} in methanol.[44] Dihydrotanshinone I (Quality Phytochemicals LLC; 98% pure by high-performance liquid chromatography) gave an ε_{409} of 3400 M^{-1} cm^{-1} in methanol based on the concentration by weight. Territrem B was isolated from the culture broth of arisugacin-producing strain *Penicillium* sp. FO-4259.[45] An ε_{331} of 18400 M^{-1} cm^{-1} in methanol[39] was assumed. The uncharged inhibitors were dissolved at concentrations of 1−3 mM in methanol, although in several experiments dihydrotanshinone I was dissolved at a concentration of 25 mM in DMSO before dilution in methanol to ensure solubility on further dilution into assays.

Assay of Substrate Hydrolysis. The substrate was AcSCh in all assays, and hydrolysis rates (v) were measured in a coupled Ellman reaction in which the amount of thiocholine generated in the presence of 0.33 mM DTNB was determined by the formation of the thiolate dianion of DTNB at 412 nm ($\Delta\varepsilon_{412}$ = 14150 M^{-1} cm^{-1}).[20] Total AChE concentrations (E_{tot}) were calculated assuming 450 units/nmol.[7,b] Assays were conducted at 25 °C in 20 mM sodium phosphate buffer (pH 7.0) (stock buffer) and 0.01% bovine serum albumin[46] unless otherwise noted. AChE concentrations were varied to optimize measured rates, and nonenzymatic hydrolysis rates were deducted from all enzymatic hydrolysis rates.

The fitting of kinetic data with AChE inhibitors was conducted by nonlinear regression with SigmaPlot (version 11.0), and analyses were either unweighted (eqs 1 and 4) or weighted assuming that the dependent variable had a constant percent error[47] (eqs 2, 3, 5, 6A, 6B, and 7A) unless otherwise noted.

Inhibition of Substrate Hydrolysis at Low Substrate Concentrations. To simplify the analysis of inhibition of substrate hydrolysis arising from the interaction of ligands with either the A- or P-site in only the free enzyme (E), it is useful to focus on the second-order hydrolysis rate constant obtained when the substrate concentration ([S]) is much less than K_{app}, the apparent Michaelis constant.[42] Here we denote this rate constant k_E.[42,48] In the absence of inhibitors, $k_E = k_{cat}/K_{app}$, where k_{cat} is the turnover number for the substrate with AChE.[19] Under these conditions, Scheme 1 includes all relevant

Scheme 1. Enzyme Species Considered in the Low-Substrate Kinetic Model

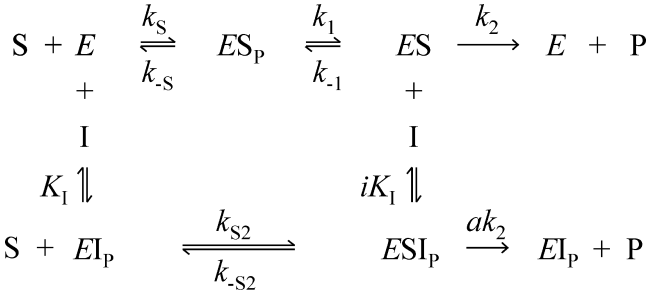

enzyme species.[42] This scheme assumes that substrate S binds initially to the P-site (ES_P) before progressing to the A-site (ES) where it is hydrolyzed to products P, and it can be applied both to inhibitors that bind at the A-site (I_P = I, and $1/i$ = 0) and to inhibitors that bind at the P-site (I_P) with dissociation constant K_I. Under these second-order conditions, the substrate hydrolysis rate $v = k_E[E]_{tot}[S]$, where $[E]_{tot}$ is the total enzyme concentration and k_E is measured from eq 1.[49]

$$[S] = [S]_0 e^{-zt} \quad (1)$$

In eq 1, $z = k_E[E]_{tot}$ and t is the time after addition of S to the complete assay mixture. To fit hydrolysis data, the following substitutions were made in eq 1 and the equation was solved for A_{412} at time t: $[S] = [A_{412} - A_{412(final)}]/\Delta\varepsilon_{412}$, where $A_{412(final)}$ is A_{412} at the conclusion of the exponential time course, and $[S]_0 = [A_{412(final)} - A_{412(t=0)}]/\Delta\varepsilon_{412}$.[46]

Because AcSCh is hydrolyzed by AChE at nearly diffusion controlled rates, binding of the inhibitor to either the A- or P-site results in an expression for the ratio of k_E in the absence of inhibitor ($k_{E[I]=0}$) to k_E in the presence of inhibitor (k_{E+I}) given by eq 2.[22]

$$\frac{k_{E[I]=0}}{k_{E+I}} = \frac{1 + \frac{[I]}{K_I}}{1 + \frac{\alpha[I]}{K_I}} \quad (2)$$

Under these diffusion-controlled conditions, α in eq 2 is given by k_{S2}/k_S, from Scheme 1 the ratio of the association rate constant for S with EI_P to the association rate constant for S with E.[42] The value of α is always zero for inhibitors that bind specifically to the A-site because k_{S2} then is zero, and it is expected to be close to zero when the bound P-site ligand blocks the entry of AcSCh into the A-site.[18,22,42]

To conduct an inhibitor competition assay, two inhibitors for which α = 0 are selected. A series of assays are then conducted with a fixed concentration of one inhibitor (I1) together with varying concentrations of the second inhibitor (I2), and k_E in the presence of both inhibitors (here denoted k_{E+I2}) relative to k_E when only I1 is present (here denoted $k_{E[I2]=0}$) is given by eq 3.[7]

$$\frac{k_{E+I2}}{k_{E[I2]=0}} = \frac{K_2\left(1 + \frac{[I1]}{K_1}\right)}{K_2\left(1 + \frac{[I1]}{K_1}\right) + [I2]\left(1 + \frac{[I1]}{K_{12}}\right)} \quad (3)$$

In eq 3, K_1, K_2, and K_{12} are the equilibrium dissociation constants for I1 with E, I2 with E, and I1 with the EI2 complex, respectively. The value of $[I1]/K_{12}$ will be significantly greater than zero only if the ternary complex EI1I2 can form, and this analysis thus can be used to detect ternary complex formation.

Inhibition of Substrate Hydrolysis at Intermediate Substrate Concentrations. At substrate concentrations that are near K_{app} but low enough that highly substrate bound species can be ignored (e.g., ESS_P[20]), an acyl enzyme intermediate (EA) in addition to those in Scheme 1 must be considered. In this report, these concentrations are used with only one inhibitor, territrem B, that we will show is unable to form ternary complexes with ligands that bind specifically to either the A- or P-site. Under these conditions, Scheme 2 includes all relevant enzyme species.[c] Inhibitor I spans the A- and P-sites and binds to E with respective association and dissociation rate constants k_I and k_{-I} and to EA with respective association and dissociation rate constants k_{AI} and k_{-AI}.

Scheme 2. Enzyme Species Considered at Intermediate Substrate Concentrations

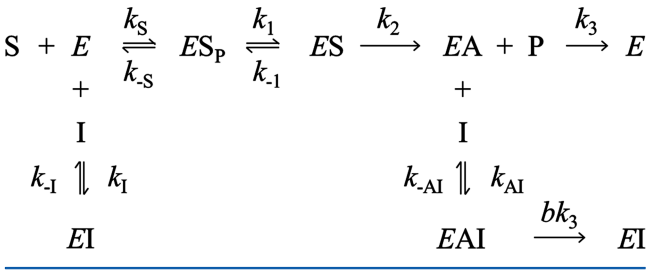

When the concentration of a slow binding inhibitor in Scheme 2 is changed at the start of an AChE assay containing the substrate AcSCh, a continuous trace of A_{412} versus t can be recorded as the assay approaches a new steady state. If substrate is only minimally depleted and the absorbance and time scales are adjusted so that the trace would be linear in the absence of inhibitor, we observe that the trace with inhibitor can be analyzed with eq 4.

$$A_{412} = A_{t=0} + v_{final}t + \left(\frac{v_0 - v_{final}}{k_{obs}}\right)(1 - e^{-k_{obs}t}) \quad (4)$$

In eq 4, $A_{t=0}$ is A_{412} at time zero, v_0 and v_{final} are the hydrolysis rates dA_{412}/dt at time zero and the final steady state, respectively, and k_{obs} is the observed rate constant for the approach to the final steady state. In cases where $v = dA_{412}/dt$ rather than A_{412} was measured, data were fit to the time derivative of eq 4 shown in eq 5.

$$v = v_{final} + (v_{initial} - v_{final})e^{-k_{obs}t} \quad (5)$$

The general expression for v_{final} that arises from Scheme 2, when I is not necessarily in equilibrium with EA, has been derived previously[1,41] and is given in a rearranged format in eqs 6A and 6B.

$$\frac{v_{[I]=0}}{v_{final+I}} = 1 + \frac{[I]}{K_{I\,app}} \quad (6A)$$

$$K_{I\,app} = \frac{K_I\left(1 + \frac{[S]}{K_{app}}\right)}{1 + \frac{K_I[S]}{K_U K_{app}}} \quad (6B)$$

When v_{final} in the presence of I ($v_{final+I}$) is normalized to v in the absence of I ($v_{[I]=0}$), a plot of $v_{[I]=0}/v_{final+I}$ versus [I] is linear when [S] approaches zero with a slope that gives the apparent K_I ($K_{I\,app}$) = K_I. As [S] increases, $K_{I\,app}$ becomes a function of [S] and depends on the ratio $K_I/K_U = (k_{cat}/k_3)K_I(1 - b + bk_3/k_{-I})/(K_R + b[I])$, where $K_R = (k_{-AI} + bk_3)/k_{AI}$.[41] The value of this ratio in turn depends on whether I is in equilibrium with E and EA: at equilibrium ($bk_3 \ll k_{-I}$, and $bk_3 \ll k_{-AI}$), $K_R = K_{AI}$ and the extent of inhibition depends on the value of b.[22] With a very slow-binding inhibitor like territrem B, Scheme 2 is not at equilibrium ($bk_3 \gg k_{-I}$, and $bk_3 \gg k_{-AI}$). If $v_{[I]=0}/v_{final+I}$ remains linear in [I], implying K_I/K_U is independent of [I] ($k_3/k_{AI} \gg$ [I]), then $K_I/K_U = (k_{cat}/k_3)(k_{AI}/k_I)$.[41] The ratio k_{cat}/k_3 is a measure of the fraction of total substrate-bound enzyme intermediates in the acetyl enzyme form $[EA]/([ES_P] + [ES] + [EA])$.

The approach to the steady state in eq 4 involves only a single-exponential term (k_{obs}), and conditions have been described previously[50] under which this situation can arise from Scheme 2. Either one inhibitor-bound species predominates (e.g., $[EI] \gg [EAI]$), or inhibitor dissociation is essentially unaffected by enzyme acetylation ($k_{-I} \cong k_{-AI}$). The resulting expression for k_{obs} in eq 4 is given in eqs 7A and 7B.

$$k_{obs} = k_{on}([I] + K_{I\,app}) \quad (7A)$$

$$k_{on} = \frac{k_I\left(1 + \frac{k_{cat}k_{AI}[S]}{k_3k_IK_{app}}\right)}{1 + \frac{[S]}{K_{app}}} \quad (7B)$$

RESULTS

Aflatoxin B1. Our search for uncharged inhibitors with binding specificity for the AChE P-site began with aflatoxin B1, the first uncharged inhibitor shown by X-ray crystallography to bind specifically to the P-site.[31] To demonstrate that our inhibitor competition assay supports this assignment, we conducted the analyses in Figure 3. We first measured aflatoxin B1 inhibition of AChE hydrolysis of low concentrations of the substrate AcSCh. The substrate was completely hydrolyzed over an exponential time course (eq 1 and Figure 3A), and second-order, substrate hydrolysis rate constants (k_E) were obtained at several inhibitor concentrations. Such direct measurements of k_E are attractive because they are more precise than those obtained from a series of conventional initial rate measurements. Furthermore, under these second-order conditions, inhibition reflects binding of aflatoxin B1 only to the free enzyme. Values of $k_{E[I]=0}/k_{E+I}$ had a linear dependence on the aflatoxin B1 concentration (Figure 3B), providing a K_I of 28 μM and indicating that substrate reacts slowly if at all with the inhibitor-bound enzyme (α in eq 2 is zero). In this case, the inhibitor competition analysis in eq 3 can then be applied.[7,41,42] This analysis is designed to assign the binding location of an unknown inhibitor by examining its competition with inhibitors whose binding sites are known from X-ray crystallography. In Figure 3, the A-site inhibitor edrophonium[51] and the P-site inhibitor thioflavin T[11] (Figure 2) are employed as the known

dx.doi.org/10.1021/bi401043w | Biochemistry 2013, 52, 7486−7499

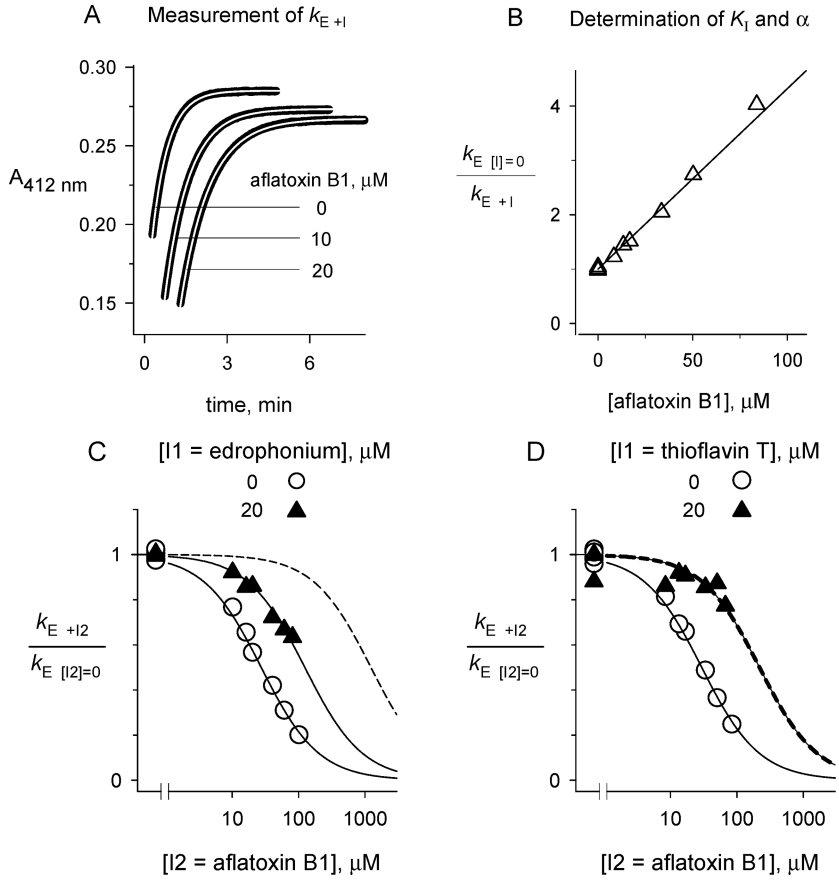

Figure 3. Inhibition of AcSCh hydrolysis by aflatoxin B1. (A) Examples of experimental traces that were analyzed with eq 1 to yield values of k_{E+I}. The assay solvent consisted of 20 mM sodium phosphate (pH 7.0), 10% methanol, and 0.02% Triton X-100. The initial AcSCh concentration ($[S]_0$) was 10 μM; $[E]_{tot}$ was 0.37 nM (for ≤20 μM I) or 0.7−1.1 nM [for ≥40 μM I (not shown)], and aflatoxin B1 concentrations are indicated. Experimental traces (black) at 0, 10, and 20 μM aflatoxin B1 and fitted lines (white) are offset by 0.02, 0.01, and 0 A_{412}, respectively, and 0, 0.5, and 1.0 min, respectively, for the sake of clarity. (B) Values of k_{E+I} obtained from traces like those in panel A were analyzed with eq 2. Weighted analysis of two data sets (n = 2) gave an α of −0.059 ± 0.010 (not significantly different from zero based on a P value of 0.11). With α fixed at zero, an average K_I of 28 ± 1 μM (n = 2) was obtained. (C and D) Inhibitor competition assay for assignment of AChE binding site specificity. Values of k_E, with inhibitor I2 in the presence (▲) or absence (○) of inhibitor I1 as indicated, were obtained as described for panel A, and the $k_{E+I2}/k_{E[I2]=0}$ ratios were fit to eq 3. Values of K_1 (0.45 ± 0.02 μM for edrophonium and 3.01 ± 0.12 μM for thioflavin T) and K_2 for aflatoxin B1 (27.1 ± 0.9 and 29.2 ± 0.9 μM in panels C and D, respectively) were obtained as described for panels A and B, and these values were fixed in eq 3 and K_{12} was fit. For edrophonium and aflatoxin B1 (C), the affinity in the binary complexes relative to that in the ternary complex was given by a K_{12}/K_1 of 5.0 ± 0.3. For thioflavin T and aflatoxin B1 (D), K_{12}/K_1 > 1000 because K_1/K_{12} was not significantly different from zero (p = 0.86). Dashed lines were calculated with the same values of K_1 and K_2 but with $[I1]/K_{12}$ fixed at zero.

inhibitors and aflatoxin B1 is analyzed as the unknown inhibitor. The analysis is designed to detect any ternary complex formed when the unknown inhibitor and the inhibitor with a known binding site are added to AChE simultaneously. The data with aflatoxin B1 alone are plotted in the form $k_{E+I}/k_{E[I]=0}$ in panels C and D of Figure 3 to emphasize K_I as the IC_{50}, or the inhibitor concentration at which $k_{E+I}/k_{E[I]=0}$ was decreased by 50%. When a fixed concentration of edrophonium was included in the assays, the IC_{50} for aflatoxin B1 was shifted slightly to the right, indicating some competition between the two inhibitors. The affinity of aflatoxin B1 or edrophonium in the ternary complex decreased by a factor of 5 relative to their affinities in their respective binary complexes with the free enzyme, a small change consistent with slight steric overlap between the two binding sites. In principle, this small decrease in affinity could also arise from a negative allosteric interaction between the two ligand binding sites, but crystal structures of the edrophonium and aflatoxin B1 complexes with *Tc*AChE show no evidence of backbone α-carbon movements necessary for an enzyme conformational change that could give rise to such allosterism.

In contrast to the results with edrophonium, the IC_{50} for aflatoxin B1 in Figure 3D was shifted well to the right by the addition of thioflavin T. One can calculate the extent of the shift that would result from complete competition and no ternary complex formation from the K_I values of the inhibitors individually, and these calculated shifts are shown as the dashed lines in panels C and D of Figure 3. Aflatoxin B1 and thioflavin T showed complete competition in Figure 3D. These data indicate that aflatoxin B1 binds to the AChE P-site in a fashion that is competitive with thioflavin T but slightly overlaps edrophonium bound at the A-site. This interpretation confirms the P-site binding of aflatoxin B1 complexed with AChE in the crystal structure of Protein Data Bank (PDB) entry 2XI4,[31] as outlined in the Discussion.

Dihydrotanshinone I. To find a more attractive uncharged lead compound as a specific P-site inhibitor of AChE, we surveyed the literature for reports of uncharged natural

dx.doi.org/10.1021/bi401043w | *Biochemistry* 2013, 52, 7486−7499

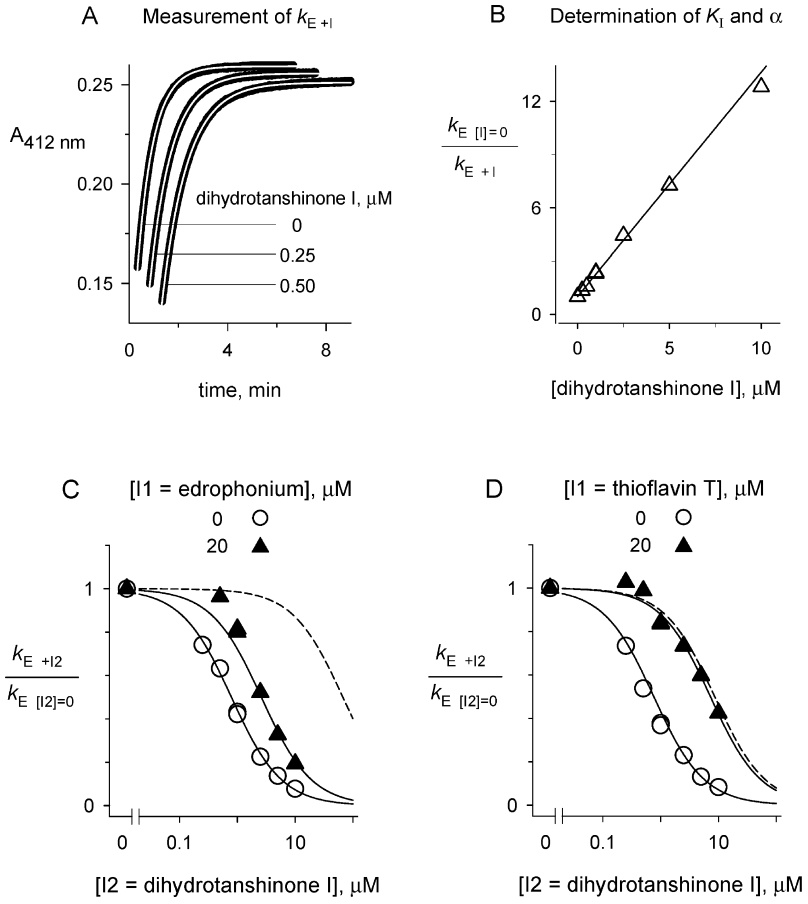

Figure 4. Inhibition of AcSCh hydrolysis by dihydrotanshinone I. (A) Examples of experimental traces that were analyzed as described in the legend of Figure 3A. The solvent was assay buffer containing 10% methanol, 0.04% DMSO, and 0.01% BSA. $[S]_0$ was 10 μM; $[E]_{tot}$ was 0.30 nM (for $\leq$0.5 μM I) or 0.5−2.7 nM [for $\geq$1.0 μM I (not shown)], and dihydrotanshinone I concentrations are indicated. Experimental traces (black) at 0, 0.25, and 0.50 μM dihydrotanshinone I and fitted lines (white) are offset by 0.006 A_{412} and 0.5 and 1.0 min, respectively, for the sake of clarity. (B) Values of k_{E+I} obtained from traces like those in panel A were analyzed with eq 2. Weighted analysis of four data sets gave an α of 0.0133 ± 0.0047 (not significantly different from zero based on a P value of 0.067). With α fixed at zero, an average K_I of 0.75 ± 0.04 μM (n = 3) was obtained. (C and D) Inhibitor competition assays for the assignment of AChE binding site specificity were conducted as described in the legend of Figure 3. Values of K_1 (0.239 ± 0.001 μM for edrophonium and 1.94 ± 0.05 μM for thioflavin T) and K_2 for dihydrotanshinone I (0.79 ± 0.02 and 0.76 ± 0.05 μM in panels C and D, respectively) were obtained as described for panels A and B, and these values were fixed in eq 3 and K_{12} was fit. For edrophonium and dihydrotanshinone I (C), the affinity in the binary complexes relative to that in the ternary complex was given by a K_{12}/K_1 of 3.4 ± 0.3. For thioflavin T and dihydrotanshinone I (D), K_{12}/K_1 = 54 ± 18. Dashed lines were calculated as described in the legend of Figure 3.

products with affinities higher than that of aflatoxin B1 as AChE inhibitors. Dihydrotanshinone I (Figure 2) was reported to be a potent inhibitor of AChE[36] with a K_I of 0.64 μM.[37] Furthermore, its planar structure with an ortho-quinone ring bore some resemblance to aflatoxin B1 and its pyrone and cyclopentenone rings (Figure 2). These features made it an attractive candidate for a specific P-site inhibitor. The analysis of dihydrotanshinone I binding to AChE with our inhibitor competition assay is shown in Figure 4. The dependence of k_E on the dihydrotanshinone I concentration (Figure 4B) gave a K_I of 0.75 μM and indicated, as in Figure 3B, that α in eq 2 is zero. The inhibitor competition assays with a fixed concentration of edrophonium revealed a slight shift to the right in IC_{50} for dihydrotanshinone I (Figure 4C). The affinity of dihydrotanshinone I or edrophonium in the ternary complex decreased by a factor of 3.4 relative to their affinities in their respective binary complexes with the free enzyme, a small change that indicated slight steric overlap between the two binding sites. In contrast, the IC_{50} for dihydrotanshinone I in Figure 4D was shifted well to the right by the addition of thioflavin T, almost to the theoretical dashed line indicating complete competition between these two inhibitors. These data indicate that dihydrotanshinone I, like aflatoxin B1, binds to the AChE P-site in a fashion that is competitive with thioflavin T but slightly overlaps edrophonium bound at the A-site.

Association and Dissociation Rate Constants of Territrem B. One class of high-affinity AChE inhibitors encompasses a number of closely related fungal meroterpenoids, including the terreulactones, arisugacins, and territrems.[52] Territrem B (Figure 2) has been reported to be an irreversible inhibitor of electric eel AChE that does not form a covalent bond with the enzyme.[39] This conclusion was based on two observations: These authors failed to detect a gradually approaching steady state in the inhibition of AChE by territrem B, yet radiolabeled territrem B was released from AChE by 8 M urea, indicating a noncovalent binding mechanism. In contrast, our data with human AChE in Figures 5 and 6 reveal high-affinity but reversible binding of territrem B. The reversibility is readily apparent in the continuous assays with AcSCh in panels A and B of Figure 5. These assays show the approach to steady

dx.doi.org/10.1021/bi401043w | *Biochemistry* 2013, 52, 7486−7499

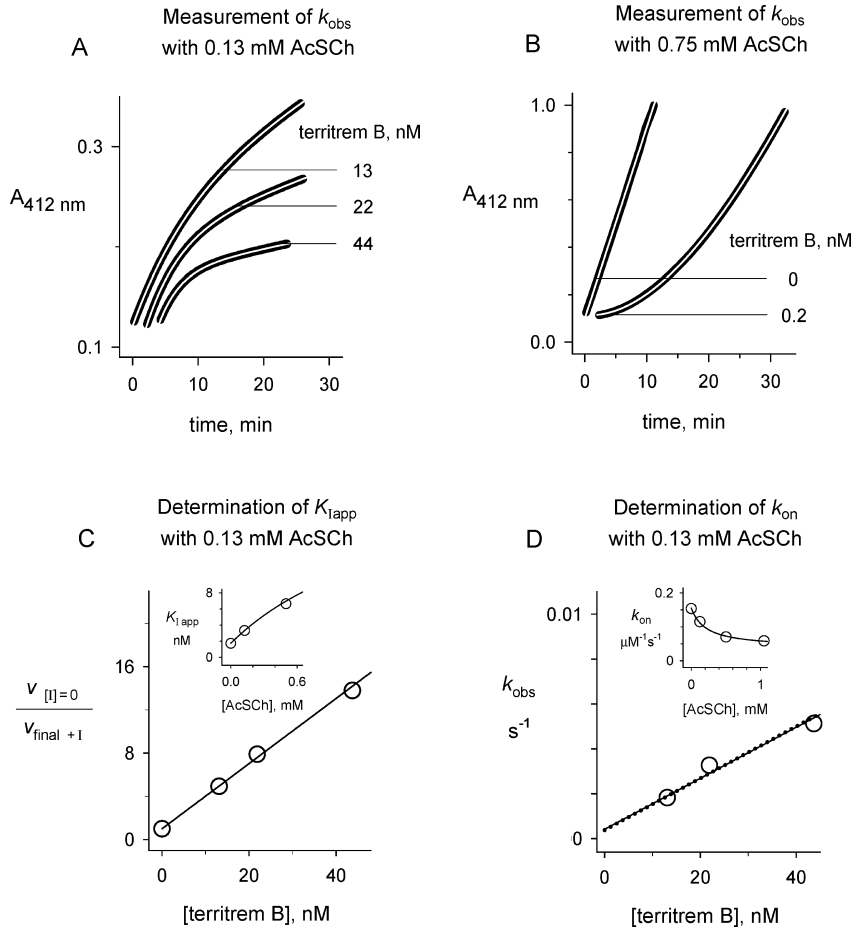

Figure 5. Association and dissociation rate constants for binding of territrem B to AChE in the presence of AcSCh. Stock buffer was supplemented with 0.02% Triton X-100 and 0.0001% BSA in the assays. (A) Samples of territrem B were added to the assays at time zero. Experimental traces were analyzed with eq 4 to obtain fitted values of four parameters, including v_{final} and k_{obs}. The concentration of substrate ($[S]_0$) was 0.125 mM; $[E]_{tot}$ was 6 pM, and territrem B concentrations are indicated. Experimental traces (black) at 13, 22, and 44 nM territrem B and fitted lines (white) are offset by 0, 2, and 4 min, respectively, for the sake of clarity. (B) A sample with territrem B (100 nM) and a control without territrem B were incubated for 3 h with AChE and diluted into assays to the indicated territrem B concentration at time zero. Analysis was the same as in panel A except that v_{final} was fixed at the control value, $[S]_0$ was 0.75 mM, and $[E]_{tot}$ was 12 pM. Experimental traces (black) at 0 and 0.2 nM territrem B and fitted lines (white) are offset by 0 and 2 min, respectively, for the sake of clarity. (C) Values of v_{final} obtained from traces in panel A were analyzed with eq 6A to obtain a $K_{I\ app}$ of 3.19 ± 0.15 nM. The $K_{I\ app}$ from this set together with those from similar analyses of v_{final} with $[S]_0$ at 0.50 mM and $[S]_0$ at 0 (Figure 5D) were analyzed with eq 6B in the inset to give fitted values of K_{app} (0.11 mM) and $(k_{cat}/k_3)(k_{AI}/k_I)$ (0.10). (D) Values of k_{obs} obtained from traces in panel A were analyzed with eq 7A to obtain a k_{on} of 0.11 ± 0.02 $\mu M^{-1}\ s^{-1}$ (—). When $K_{I\ app}$ in eq 7A is fixed at the value determined in panel C, k_{on} = 0.120 ± 0.006 $\mu M^{-1}\ s^{-1}$ (···). The k_{on} from this fit together with those from similar analyses of k_{obs} with $[S]_0$ at 1.05 and 0.50 mM and $[S]_0$ at 0 mM (Figure 6E) was analyzed in the inset with eq 7B to give fitted values of K_{app} (0.21 ± 0.07 mM), k_I (0.162 ± 0.008 $\mu M^{-1}\ s^{-1}$), and $(k_{cat}/k_3)(k_{AI}/k_I)$ (0.25 ± 0.05). Error bars in panels C and D are within the symbols.

state territrem B binding during both net association with the unoccupied enzyme (Figure 5A) and net dissociation from the complex of territrem B with AChE (Figure 5B).

While these continuous assays are convenient and qualitatively make clear both association and dissociation reactions, quantitative analyses must consider the competition between territrem B and AcSCh for binding to the enzyme active site. We modeled this competition with Scheme 2 and fit the data in panels A and B of Figure 5 with eq 4 to give the initial substrate hydrolysis rate (v_0) upon addition of enzyme to substrate, the final rate (v_{final}) when a steady state is achieved, and the exponential rate constant (k_{obs}) for the approach to the steady state. Because eq 4 assumes a constant hydrolysis rate v for a control in the absence of inhibitor (see Figure 5B), a substrate concentration is often chosen that is the lowest necessary to maintain a constant control rate while minimizing competition with the inhibitor. For example, a higher substrate concentration was employed for the net dissociation reaction in Figure 5B than for the net association reaction in Figure 5A. The dependence of v_{final} from Figure 5A on inhibitor concentration was fit with eq 6A in Figure 5C to give the apparent inhibition constant ($K_{I\ app}$). $K_{I\ app}$ reflects a weighted average of binding of the inhibitor to both free enzyme E and acyl enzyme EA in Scheme 2 and thus is dependent on the substrate concentration as given in eq 6B and shown in the inset of Figure 5C. The value of K_{app} for AcSCh obtained from this fit was 0.11 mM, in reasonable agreement with the K_{app} of 0.045 mM for AcSCh under these solvent conditions directly measured from Michaelis–Menten kinetic analysis.[22] Information about rate constants was obtained by analyzing k_{obs} values from Figure 5A. The dependence of k_{obs} on territrem B concentration in Figure 4D was fit to eq 7A with $K_{I\ app}$ both as a variable (—) and as a parameter fixed from Figure 4C (···). In this case, the resulting values of k_{on} were in very good

dx.doi.org/10.1021/bi401043w | *Biochemistry* 2013, 52, 7486–7499

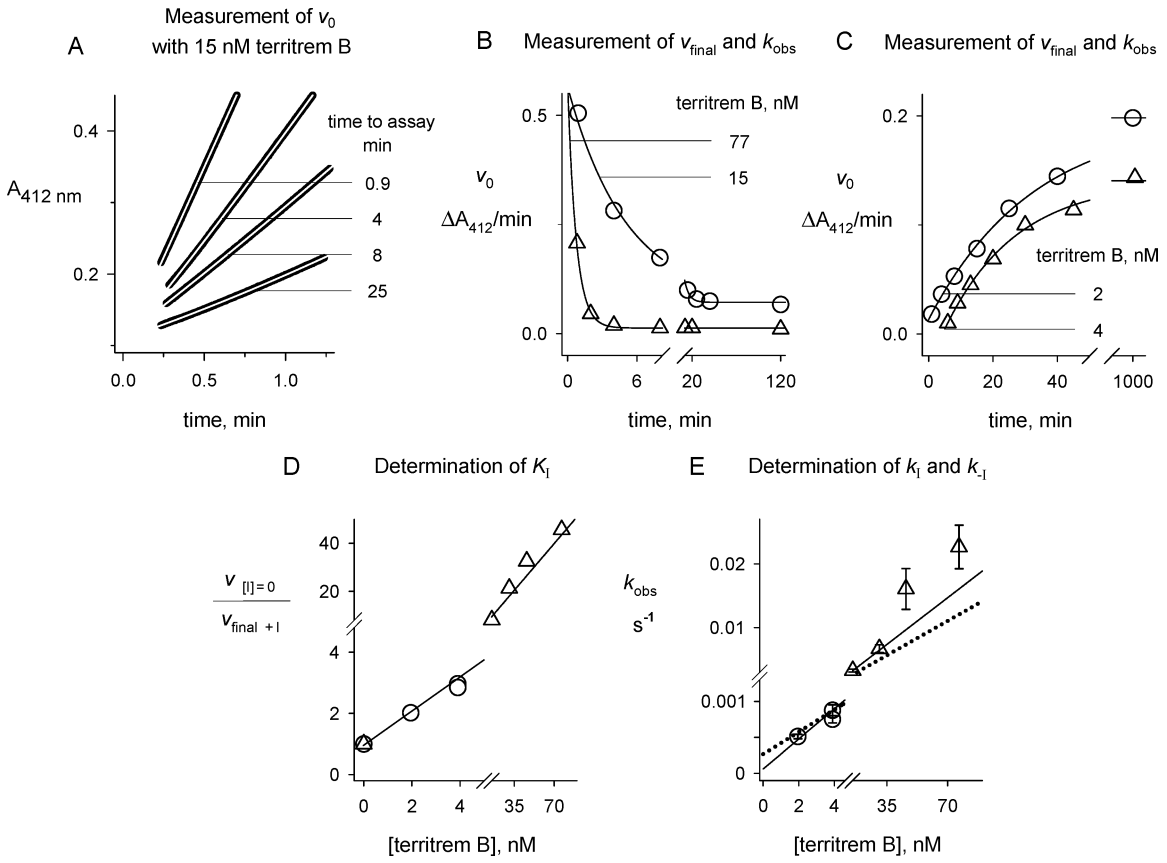

Figure 6. Association and dissociation rate constants for binding of territrem B to AChE in the absence of AcSCh. Stock buffer was supplemented with 0.02% Triton X-100 and 0.01% BSA in initial incubations and subsequent assays. (A) Samples with 15 nM territrem B and 1 nM AChE were incubated for the indicated times and diluted 10-fold into assays containing 1.05 mM AcSCh at assay time zero. Experimental traces were analyzed with eq 4 with v_{final} fixed at 0.50 ΔA_{412}/min to obtain fitted values of v_0, k_{obs}, and $A_{t=0}$. This v_{final} value was calculated with eq 6A from the control v without inhibitor and the $K_{I\ app}$ for 1.05 mM AcSCh fit in the inset of Figure 5D. Experimental traces are black, and fitted lines are white; the 4 min trace and fit are offset by 0.01 absorbance unit for the sake of clarity. (B) Values of v_0 from traces at each time point in panel A and traces at additional time points from the same incubation (○) and values of v_0 from traces from a similar incubation with 77 nM territrem B (△) were fit to eq 5 to give (for ○) v_{final} (0.072 ± 0.03 ΔA_{412}/min) and k_{obs} (0.197 ± 0.014 min^{-1}) and (for △) v_{final} (0.0127 ± 0.0010 ΔA_{412}/min) and k_{obs} (1.4 ± 0.2 min^{-1}). (C) Territrem B (380 or 190 nM) and AChE (27 nM) were incubated for 10 min and diluted 100-fold. At the indicated times, aliquots were diluted 3.3-fold into continuous assays containing 1.05 mM AcSCh, and values of v_0, k_{obs}, and $A_{t=0}$ were obtained by fitting with eq 4 as described for panel A. These values of v_0 at each time point were then analyzed with eq 5 as described for panel B to give [(○) 2 nM territrem B] v_{final} (0.198 ± 0.007 ΔA_{412}/min) and k_{obs} (0.031 ± 0.002 min^{-1}) and [(△) 4 nM territrem B] v_{final} (0.141 ± 0.005 ΔA_{412}/min) and k_{obs} (0.045 ± 0.003 min^{-1}). The 4 nM territrem B trace and fit are offset by 5 min for the sake of clarity. (D) Values of v_{final} obtained from association reactions, including those in panel B (△), and dissociation reactions, including those in panel C (○), were initially analyzed with eq 2 to obtain an α of −0.005 ± 0.003 (p = 0.19, not significantly different from zero) and then analyzed with eq 6A to yield $K_{I\ app} \equiv K_I$ = 1.67 ± 0.19 nM. Error bars in panels B–D are within the symbols. (E) Values of k_{obs} obtained from the traces analyzed in panel D were fit with eq 7A to yield $k_{on} \equiv k_I$ = 0.21 ± 0.02 μM^{-1} s^{-1} (—). When $K_{I\ app} \equiv K_I$ in eq 7A was fixed at the value determined in panel D, $k_{on} \equiv k_I$ = 0.160 ± 0.014 μM^{-1} s^{-1} (···), and $k_{-I} \equiv k_I K_I$ = 0.00027 ± 0.00004 s^{-1}. In these analyses, the dependent variable was weighted by the reciprocal of its variance.[47]

agreement, but for determinations of k_{on} at other substrate concentrations in the inset of Figure 4D, scatter in the data was reduced by fixing $K_{I\ app}$ at values based on the fitted curve in Figure 4C. Analysis of the k_{on} values in the inset of Figure 5D with eq 7B again gave the K_{app} for AcSCh among the fitted parameters, and in this case, K_{app} was 0.21 ± 0.07 mM. Agreement of this K_{app} with that from the inset of Figure 5C was within a factor of 2. A possible explanation for the slight overestimates of these K_{app} values relative to that from direct Michaelis–Menten analysis is that Scheme 2 ignores additional substrate binding in complexes like ESS_P and EAS_P,[20] and such binding would decrease the fitted K_{app}.[50]

Key measurements in the insets of panels C and D of Figure 5 are values of $K_{I\ app}$ and k_{on} in the absence of substrate, as these are the respective equilibrium dissociation constant (K_I) and the association rate constant (k_I) for the binding of territrem B to the free enzyme. To determine these values, we conducted assays at various times after mixing territrem B and AChE. In Figure 6A, mixing occurred at time zero and the incubated mixture was assayed at subsequent time points as territrem B (15 nM) progressively associated with the enzyme. Because a new steady state was introduced in the assay, assay traces were extrapolated back to assay time zero with eq 4 to obtain the correct v_0 for the corresponding incubation time. These v_0 values were then plotted against incubation time in Figure 6B and fit with eq 5. Values of v_0 for an additional mixture with 77 nM territrem B are also fit in Figure 6B. Incubations were also initiated by dilution of territrem B and AChE mixtures, and fitted v_0 values from assays as territrem B dissociated from the enzyme were analyzed in Figure 6C. Both v_{final} and k_{obs} were obtained from each fitted line in panels B and C of Figure 6, and these data together with data from additional

dx.doi.org/10.1021/bi401043w | Biochemistry 2013, 52, 7486–7499

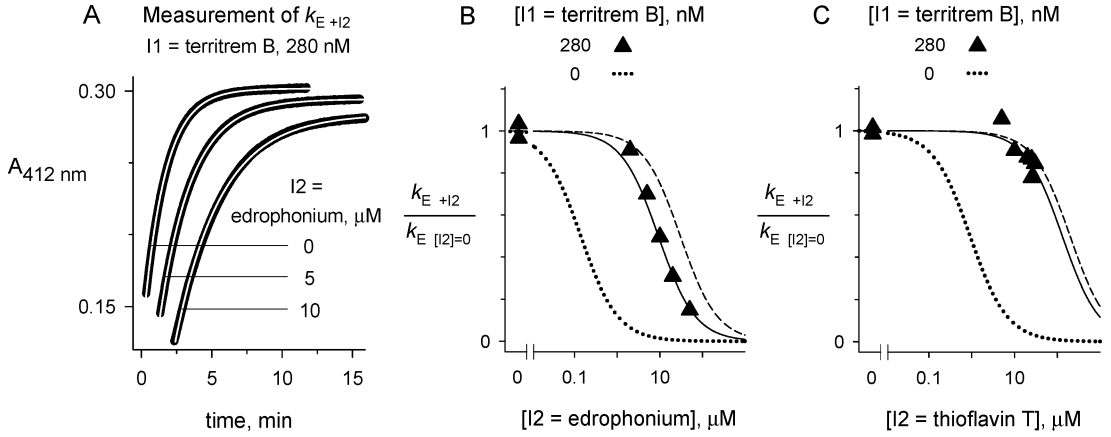

Figure 7. Inhibition of acetylthiocholine hydrolysis by territrem B. (A) Examples of experimental traces that were analyzed with eq 1 to obtain values of k_{E+I2}. The assay solvent consisted of 20 mM sodium phosphate (pH 7.0), 0.5% methanol, and 0.01% BSA. Substrate S was acetylthiocholine ($[S]_0$ = 10 μM). I1 was territrem B (280 nM). $[E]_{tot}$ was 13 nM (for ≤10 μM I2) or 25−50 nM [for >10 μM I2 (not shown)]. Edrophonium (I2) concentrations are indicated. The assay mixture with the enzyme was incubated for 15 min after addition of I1 and an additional 15 min after addition of I2, and DTNB and finally S were added. Experimental traces (black) at 0, 5, and 10 μM edrophonium and fitted lines (white) are offset by 0.03, 0.01, and 0 A_{412}, respectively, and 0, 1, and 2 min, respectively, for the sake of clarity. (B and C) Inhibitor competition assays for assignment of AChE binding site specificity. Values of k_{E+I2}, with inhibitor I2 in the presence (▲) of inhibitor I1 as indicated, were obtained as described for panel A, and the $k_{E+I2}/k_{E[I2]=0}$ ratios were fit to eq 3. Values of K_2 (0.14 μM for edrophonium and 0.92 μM for thioflavin T, corresponding to dotted lines) and K_1 for territrem B (1.26 nM) were obtained in this solvent as described in the legends of Figures 3 and 6, respectively (not shown), and these values were fixed in eq 3 and K_{12} was fit. For edrophonium and territrem B (B), the affinity in the binary complexes relative to that in the ternary complex was given by K_{12}/K_1 = 94 ± 6. For thioflavin T and territrem B (C), K_{12}/K_1 = 411 ± 180 [K_1/K_{12} was not significantly different from zero (p = 0.056)]. Dashed lines were calculated with the same values of K_1 and K_2 but with $[I1]/K_{12}$ fixed at zero.

incubations not shown were investigated in panels D and E of Figure 6. Analysis of v_{final} in Figure 6D revealed a K_I of 1.67 nM, while fitting of k_{obs} with K_I fixed at 1.67 nM in Figure 6E gave a k_I of 0.160 μM^{-1} s^{-1} and a k_{-I} of 0.00027 s^{-1}. This value of k_I is in good agreement with the value of 0.01 nM^{-1} min^{-1} reported for electric eel AChE.[39] However, the K_I for eel AChE appears to be several-fold lower than that determined here,[39] implying a lower k_{-I} for eel AChE that could increase the incubation time needed to reach the steady state during territrem B association to the point where these authors concluded that no steady state exists.

Inhibitor Competition with Territrem B. Having established the equilibrium affinity for territrem B in Figure 6, we returned to inhibitor competition assays to examine the overlap of territrem B with the P- and A-sites. Because of the slow approach of TB to equilibrium binding, we first incubated AChE with territrem B at a concentration well in excess of the K_I for territrem B and then further incubated AChE with varying concentrations of competing inhibitor edrophonium or thioflavin T. Examples of the resulting second-order hydrolysis curves for AcSCh with edrophonium are shown in Figure 7A. These inhibitor competition assays can again be analyzed with eq 4, and the fitted curve in Figure 7B revealed a major shift to the right in IC_{50} for edrophonium relative to the curve (···) and IC_{50} calculated for edrophonium alone under these solvent conditions. The affinity of territrem B or edrophonium in the ternary complex decreased by a factor of 94 relative to their affinities in their respective binary complexes with the free enzyme, a large change that indicated almost complete steric overlap between the binding sites for these two ligands. The IC_{50} for thioflavin T in Figure 7C was also shifted well to the right in the presence of territrem B, and it was not significantly different from that for the theoretical dashed line representing complete competition between these two inhibitors. These data indicate that the binding of territrem B, unlike that of dihydrotanshinone I and aflatoxin B1, completely overlaps with the AChE P-site and also overlaps with much of the A-site occupied by edrophonium.

DISCUSSION

The Inhibitor Competition Assay Correctly Predicts the Binding Site Specificity of Three Uncharged Inhibitors of AChE. To target the AChE P-site with ligands and potential drugs that may selectively restrict access of substrates and OPs to the AChE A-site, much more information must be gathered about the structure−activity relationships of ligands that bind specifically to the P-site. We apply here an inhibitor competition assay that can correctly determine whether an AChE inhibitor binds to the P-site, the A-site, or both. The assay requires inhibitor standards known to bind exclusively to the P-site or to the A-site from known three-dimensional structures of their complexes with AChE. We selected thioflavin T as the P-site standard and edrophonium as the A-site standard, as their respective structures are known from X-ray crystallography[11,51] and superposition of the bound inhibitors shows no overlap.[11] The assay measures the affinity of a test inhibitor in a binary complex with the free enzyme relative to its affinity in ternary complexes with the inhibitor standard bound to AChE. This relative affinity is denoted by the ratio K_{12}/K_1. When the binding sites for the test inhibitor and the inhibitor standard strongly overlap, no ternary complex can form and K_{12} becomes very large relative to K_1. Conversely, when the binding sites for the test inhibitor and inhibitor standard do not overlap at all, K_{12} will approach K_1. A good example of this case is the competition assay involving the two inhibitor standards themselves, thioflavin T and edrophonium. The measured K_{12}/K_1 for this pair is 0.81 ± 0.04[42] (Table 1), confirming no overlap in binding sites in this assay and in fact suggesting a slight energetically favorable interaction between these two inhibitors in the ternary complex. Competition assay

dx.doi.org/10.1021/bi401043w | Biochemistry 2013, 52, 7486−7499

Table 1. Affinities of Inhibitors in a Binary Complex with Free Human AChE (K_1) Relative to Their Affinities in a Ternary Complex with Edrophonium Bound to the A-Site, Denoted K_{12}/K_1

inhibitor	K_1 (nM)	K_{12}/K_1	reference	
			K_{12}/K_1	crystal structure
A-site specific				
Huprine X	0.026	>1000	41	56
P-site specific				
thioflavin T	1000	0.81 ± 0.04	42	11
propidium	660	3.4 ± 0.1	this report	12
methylene blue	110	3.3 ± 0.3	23	57
aflatoxin B1	28000	5.0 ± 0.3	this report	31
dihydrotanshinone I	750	3.4 ± 0.3	this report	53
binds to both sites				
territrem B	1.7	94 ± 6	this report	53

results with several other inhibitors and edrophonium as the A-site inhibitor standard are also listed in Table 1. These results are entirely consistent with structures of the inhibitor−AChE complexes determined by X-ray crystallography. On the basis of these structures, the inhibitors in Table 1 are assigned as A-site or P-site specific or as binding to both sites. Because of our focus on P-site inhibitors, only one A-site specific inhibitor, huprine X, is included in Table 1 as a control. The K_{12}/K_1 for huprine X and edrophonium is >1000, as expected when both inhibitors bind to the A-site. Four inhibitors in addition to thioflavin T in Table 1 bind at the P-site as determined by X-ray crystallography, and these inhibitors all gave measured values of K_{12}/K_1 between 3.3 and 5.0 with edrophonium as the inhibitor standard. This result is somewhat unexpected. Propidium and methylene blue are cationic, while aflatoxin B1 and dihydrotanshinone I are uncharged; one might have expected some increase in K_{12}/K_1 just from charge interaction between a cationic inhibitor and edrophonium. Apparently, binding to the enzyme neutralizes any charge interaction. All four of these inhibitors showed high values of K_{12}/K_1 with thioflavin T as the inhibitor standard (data not shown in Table 1, but see Figures 3 and 4), consistent with their specificity for the P-site.

To examine in greater detail the binding site for the uncharged P-site specific inhibitors in Table 1, the crystal structure of aflatoxin B1 complexed with *Tc*AChE (PDB entry 2XI4) is shown in Figure 8. As in Figure 1B, the P- and A-sites are identified by color-coded acetylcholine molecules superimposed from the crystal structure of PDB entry 2HA4. Bound aflatoxin B1 overlaps with the superimposed acetylcholine molecule at the P-site. The molecular structure of aflatoxin B1 includes two nearly coplanar carbonyl groups in the adjacent pyrone and cyclopentenone rings that are potential hydrogen bond acceptors (Figures 2 and 9). In the crystal structure, the pyrone carbonyl oxygen forms hydrogen bonds with backbone amide NH groups of F295 and R296 while the cyclopentenone carbonyl oxygen H-bonds to the hydroxyl side chain of S293.[a] It appears that these are the only two backbone amide NH groups accessible for hydrogen bonding in the P-site. The aryl and cyclopentenone rings in aflatoxin B1 insert between the aryl side chains of W286 and Y341, with which they form $\pi-\pi$ stacking interactions, and water-mediated H-bonding is observed between the benzofuran oxygen and the side chain hydroxyl of Y72 and between the dihydrofuran oxygen and the side chain of Y124 (Figure 9). Crystal structures of the dihydrotanshinone I and territrem B complexes with human AChE have recently been obtained.[53] Important contacts

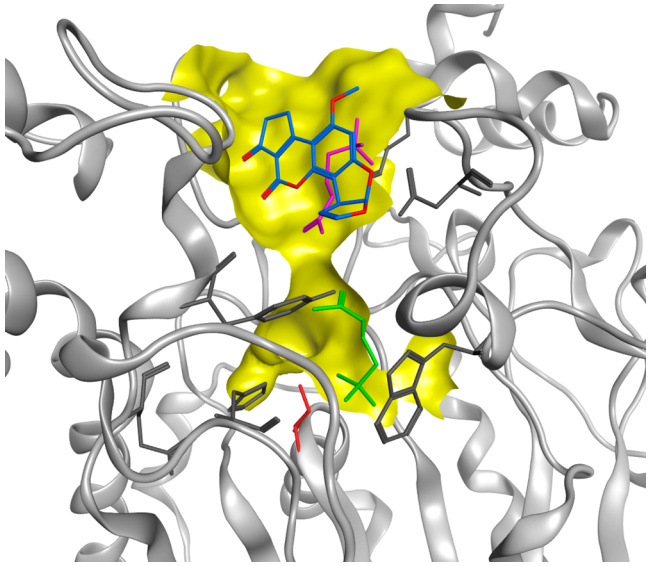

Figure 8. Crystal structure from PDB entry 2XI4 of the complex of *Tc*AChE with aflatoxin B1.[31] Aflatoxin B1 in PDB entry 2XI4 is shown, with carbon atoms colored blue and oxygens colored red. To highlight the AChE P- and A-sites, acetylcholine molecules from the crystal structure of PDB entry 2HA4 are superimposed in pink and green, respectively. The orientation of the AChE structure is identical to that in panels A and B of Figure 1.

between these bound inhibitors and P-site residues are also shown in Figure 9, and it is noteworthy that many of these contacts are similar to those in the complex of aflatoxin B1 with *Tc*AChE. All three inhibitors have aromatic groups involved in $\pi-\pi$ stacking between W286 and Y341; all three have ether oxygens that form hydrogen bonds with tyrosine hydroxyls, and aflatoxin B1 and dihydrotanshinone I have carbonyl oxygens that form hydrogen bonds with F295. However, dihydrotanshinone I and aflatoxin B1 do not extend past Y337 into the A-site while territrem B does. This explains why dihydrotanshinone I and aflatoxin do not compete significantly with edrophonium for binding to the A-site while territrem B does (Table 1). Structural features of territrem B important for its inhibition of AChE were identified by analysis of inhibitory activities of territrem B derivatives.[54] Further information was obtained in a computational docking study of arisugacin A, a related natural product that differs only in having one fewer methoxy substituent on the aryl group than territrem B. This docking of arisugacin A with AChE used two versions of

dx.doi.org/10.1021/bi401043w | *Biochemistry* 2013, 52, 7486−7499

Table 2. Rate Constants for Binding of Ligands to AChE

inhibitor	enzyme source	k_1 (μM^{-1} s^{-1})	k_{-1} ($\times 10^4$ s^{-1})	K_I (nM)	reference
monoquaternary					
edrophonium	mouse	130	320000	250	58
N-methylacridinium	mouse	850	2700000	310	58
bisquaternary					
decamethonium	mouse	230	1100000	460	58
BW286C51	mouse	450	9200	2	58
ambenonium	human	52	130	0.12	50
tertiary/primary amine					
tacrine	mouse	130	23000	18	58
huperzine A	human	0.083	3.8	4.6	22
uncharged					
coumarin	mouse	45	4200000	9300	58
territrem B	human	0.15	2.7	1.7	this work

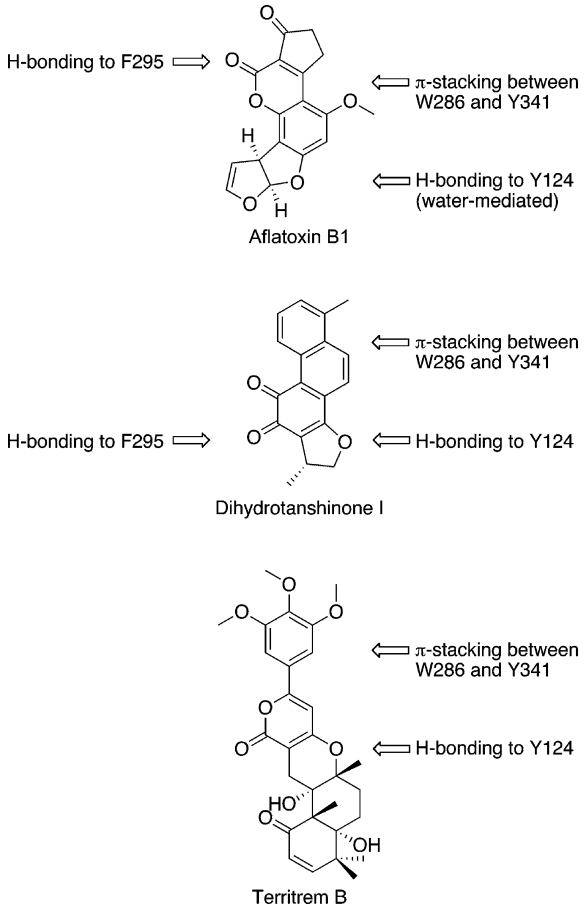

Figure 9. Molecular structures of AChE inhibitors with side chain contacts identified in the three-dimensional structures of their complexes with AChE.[a] The structures are oriented as in Figure 2.

AutoDock and found three modes of binding, one of which was favored by the authors and closely matched the binding mode subsequently observed in the crystal structure.[40] This mode has the terminal enone ring extending into the A-site. The other two docking modes both had the inhibitor rotated nearly 180° with this enone ring directed toward the mouth of the active site gorge. Despite the extent to which all three of these bound inhibitors are superimposed in the crystal structures, their AChE affinities range over 4 orders of magnitude (Table 1). The molecular basis of this variation is unclear, although the interaction of the enone ring in territrem B with the A-site clearly makes an important contribution to the higher affinity of this inhibitor.

Slow Association of Territrem B with AChE. The binding of territrem B to AChE also may be providing information about the conformational flexibility of the AChE active site gorge. Territrem B is unusual in having a very low association rate constant with AChE. The only other AChE inhibitor with a similar low association rate constant is (−)-huperzine A, which is known from X-ray crystallography to bind to the A-site.[55] The k_1 values for these two inhibitors in Table 2 are at least 300-fold lower than those for any other inhibitor in the table, regardless of whether the inhibitor is a mono- or bisquaternary ammonium ion, a tertiary amine, or an uncharged compound. It was earlier suggested that a flipped conformation of the G120 peptide bond, observed in the *Tc*AChE−(−)-huperzine A structure, might be necessary for the binding of (−)-huperzine A to AChE.[55] It was thus reasonable to speculate that the flipping process might be relatively slow and thus serve as the rate-limiting step in the association of (−)-huperzine A with AChE.[56] However, this conformational flip at G120 is not observed in the human AChE−territrem B complex.[53] Thus, the low association rate constant for territrem B must arise from another source. The crystal structure of the human AChE−territrem B complex does show a distortion of the active site gorge, particularly in regions near the P-site, with movements of backbone α-carbons of as much as 1.5 Å.[53] These regions must be at least a subset of the conformationally variable residues that allow for ligand entry, and concerted movement of these regions necessary to accommodate territrem B may be rate-limiting for territrem B association.

Territrem B Associates Almost As Well with the Acetyl Enzyme As with Free AChE. The high affinity of territrem B for AChE and its relatively low association rate constant result in low dissociation rate constants for its complexes with both free AChE and the acetyl enzyme intermediate (Figures 5 and 6). However, how much of an effect does acetylation have on territrem B binding? Some insight may be gained by recognizing a useful feature of Scheme 2, namely that algebraic expressions for the kinetic constants can be obtained without assuming any equilibria among the enzyme intermediates.[1] While the analysis in Figure 5 was not intended to present a detailed description of the effects of AcSCh on territrem B binding, some general conclusions can be drawn. The very low dissociation rate constant for territrem B with AChE is likely to keep inhibitor binding to *EA* far from equilibrium. The

dx.doi.org/10.1021/bi401043w | *Biochemistry* 2013, 52, 7486−7499

resulting expression for K_I/K_U in eq 6B[d] simplifies to $K_I/K_U = (k_{cat}/k_3)(k_{AI}/k_I)$, and therefore, k_{AI}/k_I can be determined from both the steady state and the pre-steady state analyses in the insets of panels C and D of Figure 5, respectively (see Experimental Procedures). These determinations depend on factoring out the contribution of k_{cat}/k_3, which has been estimated to be 0.5.[22] This leaves k_{AI}/k_I ratios of 0.2 and 0.5 from panels C and D of Figure 5, respectively. The agreement between the two values is reasonable, indicating that these analyses within Scheme 2 are internally consistent and that acetylation of the enzyme in the *E*A intermediate has at most a small effect on the association of territrem B with AChE. In this interpretation of Scheme 2, however, no information is obtained about the relative magnitude of dissociation rate constant k_{-AI}. When deacetylation of *E*AI is much faster than inhibitor dissociation ($bk_3 \gg k_{-AI}$), the product of k_{on} and $K_{I\ app}$ (from eqs 6B and 7B) is just k_{-I} at all substrate concentrations.

AUTHOR INFORMATION

Corresponding Author

*Mayo Clinic, 4500 San Pablo Rd., Jacksonville, FL 32224. E-mail: rosenberry@mayo.edu. Phone: (904) 953-7375. Fax: (904) 953-7370.

Funding

This work was supported by Contract HDTRA1-11-C-0017 from the U.S. Department of Defense.

Notes

The authors declare no competing financial interest.

ABBREVIATIONS

AChE, acetylcholinesterase; AcSCh, acetylthiocholine iodide; BSA, bovine serum albumin; DTNB, 5,5′-dithiobis(2-nitrobenzoic acid); OPs, organophosphates; *Tc*AChE, *Torpedo californica* AChE.

ADDITIONAL NOTES

[a]Throughout this paper, we number amino acid residues according to the human AChE sequence (Uniprot entry P22303).

[b]One unit of AChE activity corresponds to 1 μmol of acetylthiocholine hydrolyzed per minute under standard pH-stat assay conditions at pH 8.[7] Our conventional spectrophotometric assay at 412 nm[20] is conducted in pH 7 buffer. With recombinant human AChE and 0.5 mM acetylthiocholine, this assay results in 4.8 ΔA_{412}/min with 1 nM AChE or ~76% of the pH-stat assay standard.

[c]In the general steady state formulation of Scheme 2, $k_E \equiv k_{cat}/K_{app} = (k_S k_1 k_2)/(k_{-S}k_{-1} + k_2 k_{-S} + k_2 k_1)$,[18] $k_{cat} = [(k_{-1} + k_2)/(k_1 k_2) + 1/k_2 + 1/k_3]^{-1}$, and $K_{app} = (k_3/k_S)[k_1 k_2 + k_{-S}(k_{-1} + k_2)]/[k_1 k_2 + k_3(k_{-1} + k_1 + k_2)]$.

[d]At 0.5 mM AcSCh, the plot corresponding to Figure 5C is linear to 200 nM territrem B, indicating from eq 6B that $k_3/k_{AI} \gg [I]$. Because $k_3 \cong 10^4\ s^{-1}$,[22] $k_{-I} = 2.7 \times 10^{-4}\ s^{-1}$ from Figure 6E, and b is unlikely to be smaller than 10^{-6}, then $bk_3 \gg k_{-I}$ and presumably $bk_3 \gg k_{-AI}$. Then $K_I/K_U = (k_{cat}/k_3)(k_{AI}/k_I)$.

REFERENCES

(1) Rosenberry, T. L. (1975) Acetylcholinesterase. In *Advances in Enzymology* (Meister, A., Ed.) pp 103−218, John Wiley & Sons, New York.

(2) Hoffman, B. B., and Taylor, P. (2001) Neurotransmission: The autonomic and somatic motor nervous systems. In *Goodman & Gilman's The Pharmacological Basis of Therapeutics* (Hardman, J. G., Limbird, L. E., and Gilman, A. G., Eds.) pp 115−153, McGraw-Hill, New York.

(3) Giacobini, E. (2000) Cholinesterase inhibitors: From the Calabar bean to Alzheimer therapy. In *Cholinesterases and cholinesterase inhibitors. From molecular biology to therapy* (Giacobini, E., Ed.) pp 181−222, Martin Dunitz, London.

(4) Millard, C. B., and Broomfield, C. A. (1995) Anticholinesterases: Medical applications of neurochemical principles. *J. Neurochem. 64*, 1909−1918.

(5) Changeux, J.-P. (1966) Responses of acetylcholinesterase from *Torpedo marmorata* to salts and curarizing drugs. *Mol. Pharmacol. 2*, 369−392.

(6) Taylor, P., and Lappi, S. (1975) Interaction of fluorescence probes with acetylcholinesterase. The site and specificity of propidium binding. *Biochemistry 14*, 1989−1997.

(7) De Ferrari, G. V., Mallender, W. D., Inestrosa, N. C., and Rosenberry, T. L. (2001) Thioflavin T is a fluorescent probe of the acetylcholinesterase peripheral site that reveals conformational interactions between the peripheral and acylation sites. *J. Biol. Chem. 276*, 23282−23287.

(8) Rosenberry, T. L., Sonoda, L. K., Dekat, S. E., Cusack, B., and Johnson, J. L. (2008) Analysis of the reaction of carbachol with acetylcholinesterase using thioflavin T as a coupled fluorescence reporter. *Biochemistry 47*, 13056−13063.

(9) Sussman, J. L., Harel, M., Frolow, F., Oefner, C., Goldman, A., Toker, L., and Silman, I. (1991) Atomic structure of acetylcholinesterase from *Torpedo californica*: A prototypic acetylcholine-binding protein. *Science 253*, 872−879.

(10) Harel, M., Quinn, D. M., Nair, H. K., Silman, I., and Sussman, J. L. (1996) The X-ray structure of a transition state analog complex reveals the molecular origins of the catalytic power and substrate specificity of acetylcholinesterase. *J. Am. Chem. Soc. 118*, 2340−2346.

(11) Harel, M., Sonoda, L. K., Silman, I., Sussman, J. L., and Rosenberry, T. L. (2008) The crystal structure of thioflavin T bound to the peripheral site of *Torpedo californica* acetylcholinesterase reveals how thioflavin T acts as a sensitive fluorescent reporter of ligand binding to the acylation site. *J. Am. Chem. Soc. 130*, 7856−7861.

(12) Bourne, Y., Taylor, P., Radic, Z., and Marchot, P. (2003) Structural insights into ligand interactions at the acetylcholinesterase peripheral anionic site. *EMBO J. 22*, 1−12.

(13) Colletier, J. P., Fournier, D., Greenblatt, H. M., Stojan, J., Sussman, J. L., Zaccai, G., Silman, I., and Weik, M. (2006) Structural insights into substrate traffic and inhibition in acetylcholinesterase. *EMBO J. 25*, 2746−2756.

(14) Bourne, Y., Radic, Z., Sulzenbacher, G., Kim, E., Taylor, P., and Marchot, P. (2006) Substrate and product trafficking through the active center gorge of acetylcholinesterase analyzed by crystallography and equilibrium binding. *J. Biol. Chem. 281*, 29256−29267.

(15) Harel, M., Kleywegt, G. J., Ravelli, R. B. G., Silman, I., and Sussman, J. L. (1995) Crystal structure of an acetylcholinesterase-fasciculin complex: Interaction of a three-fingered toxin from snake venom with its target. *Structure 3*, 1355−1366.

(16) Bourne, Y., Taylor, P., and Marchot, P. (1995) Acetylcholinesterase inhibition by fasciculin: Crystal structure of the complex. *Cell 83*, 503−512.

(17) Tara, S., Elcock, A. H., Kirchhoff, P. D., Briggs, J. M., Radic, Z., Taylor, P., and McCammon, J. A. (1998) Rapid binding of a cationic active site inhibitor to wild type and mutant mouse acetylcholinesterase: Brownian dynamics simulation including diffusion in the active site gorge. *Biopolymers 46*, 465−474.

(18) Szegletes, T., Mallender, W. D., Thomas, P. J., and Rosenberry, T. L. (1999) Substrate binding to the peripheral site of acetylcholinesterase initiates enzymatic catalysis. Substrate inhibition arises as a secondary effect. *Biochemistry 38*, 122−133.

(19) Mallender, W. D., Szegletes, T., and Rosenberry, T. L. (2000) Acetylthiocholine binds to Asp74 at the peripheral site of human acetylcholinesterase as the first step in the catalytic pathway. *Biochemistry 39*, 7753−7763.

(20) Johnson, J. L., Cusack, B., Davies, M. P., Fauq, A., and Rosenberry, T. L. (2003) Unmasking tandem site interaction in human acetylcholinesterase. Substrate activation with a cationic acetanilide substrate. *Biochemistry 42*, 5438−5452.
(21) Wilson, I. B., and Ginsburg, S. (1955) A powerful reactivator of alkylphosphate-inhibited acetylcholinesterase. *Biochim. Biophys. Acta 18*, 168−170.
(22) Szegletes, T., Mallender, W. D., and Rosenberry, T. L. (1998) Nonequilibrium analysis alters the mechanistic interpretation of inhibition of acetylcholinesterase by peripheral site ligands. *Biochemistry 37*, 4206−4216.
(23) Wildman, S. A., Zheng, X., Sept, D., Auletta, J. T., Rosenberry, T. L., and Marshall, G. R. (2011) Drug-like leads for steric discrimination between substrate and inhibitors of human acetylcholinesterase. *Chem. Biol. Drug Des. 78*, 495−504.
(24) Polya, G. (2003) *Biochemical targets of plant bioactive compounds: A pharmacological reference guide to sites of action and biological effects*, CRC Press, Boca Raton, FL.
(25) Selim, M. I. (2010) Significance of aflatoxins in rural and global health: Concern for agricultural workers. *N.C. Med. J. 71*, 438−441.
(26) Mardani, M., Rezapour, S., and Rezapour, P. (2011) Survey of aflatoxins in Kashkineh: A traditional Iranian food. *Iran Journal of Microbiology 3*, 147−151.
(27) Roebuck, B. D. (2004) Hyperplasia, partial hepatectomy, and the carcinogenicity of aflatoxin B1. *J. Cell. Biochem. 91*, 243−249.
(28) Peraica, M., Radić, B., Lucić, A., and Pavlović, M. (1999) Toxic effects of mycotoxins in humans. *Bull. W.H.O. 77*, 754−766.
(29) Cometa, M. F., Lorenzini, P., Fortuna, S., Volpe, M. T., Meneguz, A., and Palmery, M. (2005) In vitro inhibitory effect of aflatoxin B1 on acetylcholinesterase activity in mouse brain. *Toxicology 206*, 125−135.
(30) Hansmann, T., Sanson, B., Stojan, J., Weik, M., Marty, J. L., and Fournier, D. (2009) Kinetic insight into the mechanism of cholinesterasterase inhibition by aflatoxin B1 to develop biosensors. *Biosens. Bioelectron. 24*, 2119−2124.
(31) Sanson, B., Colletier, J. P., Xu, Y., Lang, P. T., Jiang, H., Silman, I., Sussman, J. L., and Weik, M. (2011) Backdoor opening mechanism in acetylcholinesterase based on X-ray crystallography and molecular dynamics simulations. *Protein Sci. 20*, 1114−1118.
(32) Li, Z. T., Yang, B. J., and Ma, G. E. (1991) Chemical studies of *Salvia miltiorrhiza* f. *alba*. *Yao Xue Xue Bao 26*, 209−213.
(33) Park, J. W., Lee, S. H., Yang, M. K., Lee, J. J., Song, M. J., Ryu, S. Y., Chung, H. J., Won, H. S., Lee, C. S., Kwon, S. H., Yun, Y. P., Choi, W. S., and Shin, H. S. (2008) 15,16-Dihydrotanshinone I, a major component from *Salvia miltiorrhiza* Bunge (Dansham), inhibits rabbit platelet aggregation by suppressing intracellular calcium mobilization. *Arch. Pharm. Res. 31*, 47−53.
(34) Jeon, S. J., Son, K. H., Kim, Y. S., Choi, Y. H., and Kim, H. P. (2008) Inhibition of prostaglandin and nitric oxide production in lipopolysaccharide-treated RAW 264.7 cells by tanshinones from the roots of *Salvia miltiorrhiza* bunge. *Arch. Pharm. Res. 31*, 758−763.
(35) Ko, J. S., Ryu, S. Y., Kim, Y. S., Chung, M. Y., Kang, J. S., Rho, M. C., Lee, H. S., and Kim, Y. K. (2002) Inhibitory activity of diacylglycerol acyltransferase by tanshinones from the root of *Salvia miltiorrhiza*. *Arch. Pharm. Res. 25*, 446−448.
(36) Ren, Y., Houghton, P. J., Hider, R. C., and Howes, M. J. (2004) Novel diterpenoid acetylcholinesterase inhibitors from *Salvia miltiorrhiza*. *Planta Med. 70*, 201−204.
(37) Wong, K. K., Ngo, J. C., Liu, S., Lin, H. Q., Hu, C., Shaw, P. C., and Wan, D. C. (2010) Interaction study of two diterpenes, cryptotanshinone and dihydrotanshinone, to human acetylcholinesterase and butyrylcholinesterase by molecular docking and kinetic analysis. *Chem.-Biol. Interact. 187*, 335−339.
(38) Ling, K. H. (1976) Study on mycotoxins contaminated in food in Taiwan. (2) Tremor inducing compounds from *Aspergillus terreus*. *Proceedings of the National Scientific Council, Republic of China 9*, 121−129.
(39) Chen, J. W., Luo, Y. L., Hwang, M. J., Peng, F. C., and Ling, K. H. (1999) Territrem B, a tremorgenic mycotoxin that inhibits acetylcholinesterase with a noncovalent yet irreversible binding mechanism. *J. Biol. Chem. 274*, 34916−34923.
(40) Al-Rashid, Z. F., and Hsung, R. P. (2011) (+)-Arisugacin A: Computational evidence of a dual binding site covalent inhibitor of acetylcholinesterase. *Bioorg. Med. Chem. Lett. 21*, 2687−2691.
(41) Camps, P., Cusack, B., Mallender, W. D., El Achab, R., Morral, J., Muñoz-Torrero, D., and Rosenberry, T. L. (2000) Huprine X is a novel high affinity inhibitor of acetylcholinesterase that is of interest for the treatment of Alzheimer's disease. *Mol. Pharmacol. 57*, 409−417.
(42) Auletta, J. T., Johnson, J. L., and Rosenberry, T. L. (2010) Molecular basis of inhibition of substrate hydrolysis by a ligand bound to the peripheral site of acetylcholinesterase. *Chem.-Biol. Interact. 187*, 135−141.
(43) Mallender, W. D., Szegletes, T., and Rosenberry, T. L. (1999) Organophosphorylation of acetylcholinesterase in the presence of peripheral site ligands: Distinct effects of propidium and fasciculin. *J. Biol. Chem. 274*, 8491−8499.
(44) Asao, T., Buchi, G., Abdel-Kader, M. M., Chang, S. B., Wick, E. L., and Wogan, G. N. (1963) Aflatoxins B and G. *J. Am. Chem. Soc. 85*, 1706−1707.
(45) Omura, S., Kuno, F., Otoguro, K., Sunazuka, T., Shiomi, K., Masuma, R., and Iwai, Y. (1995) Arisugacin, a novel and selective inhibitor of acetylcholinesterase from *Penicillium* sp. FO-4259. *J. Antibiot. 48*, 745−746.
(46) Beri, V., Auletta, J. T., Maharvi, G. M., Wood, J. F., Fauq, A. H., and Rosenberry, T. L. (2013) Hydrolysis of low concentrations of the acetylthiocholine analogs acetyl(homo)thiocholine and acetyl(nor)-thiocholine by acetylcholinesterase may be limited by selective gating at the enzyme peripheral site. *Chem.-Biol. Interact. 203*, 38−43.
(47) Rosenberry, T. L., and Bernhard, S. A. (1971) Studies of catalysis by acetylcholinesterase: Fluorescent titration with a carbamoylating agent. *Biochemistry 10*, 4114−4120.
(48) Quinn, D. M. (1987) Acetylcholinesterase: Enzyme structure, reaction dynamics, and virtual transition states. *Chem. Rev. 87*, 955−979.
(49) Eastman, J., Wilson, E. J., Cervenansky, C., and Rosenberry, T. L. (1995) Fasciculin 2 binds to a peripheral site on acetylcholinesterase and inhibits substrate hydrolysis by slowing a step involving proton transfer during enzyme acylation. *J. Biol. Chem. 270*, 19694−19701.
(50) Hodge, A. S., Humphrey, D. R., and Rosenberry, T. L. (1992) Ambenonium is a rapidly reversible noncovalent inhibitor of acetylcholinesterase with one of the highest known affinities. *Mol. Pharmacol. 41*, 937−942.
(51) Harel, M., Schalk, I., Ehret-Sabatier, L., Bouet, F., Goeldner, M., Hirth, C., Axelsen, P. H., Silman, I., and Sussman, J. L. (1993) Quaternary ligand binding to aromatic residues in the active-site gorge of acetylcholinesterase. *Proc. Natl. Acad. Sci. U.S.A. 90*, 9031−9035.
(52) Houghton, P. J., Ren, Y., and Howes, M. J. (2006) Acetylcholinesterase inhibitors from plants and fungi. *Nat. Prod. Rep. 23*, 181−199.
(53) Cheung, J., Gary, E. N., Shiomi, K., and Rosenberry, T. L. (2013) Structures of Human Acetylcholinesterase Bound to Dihydrotanshinone I and Territrem B Show Peripheral Site Flexibility. *ACS Med. Chem. Lett.*, DOI: 10.1021/ml400304w.
(54) Peng, F. C. (1995) Acetylcholinesterase inhibition by territrem B derivatives. *J. Nat. Prod. 58*, 857−862.
(55) Raves, M. L., Harel, M., Pang, Y.-P., Silman, I., Kozikowski, A. P., and Sussman, J. L. (1997) Structure of acetylcholinesterase complexed with the nootropic alkaloid, (−)-huperzine A. *Nat. Struct. Biol. 4*, 57−63.
(56) Dvir, H., Wong, D. M., Harel, M., Barril, X., Orozco, M., Luque, F. J., Muñoz-Torrero, D., Camps, P., Rosenberry, T. L., Silman, I., and Sussman, J. L. (2002) 3D structure of *Torpedo californica* acetylcholinesterase complexed with huprine X at 2.1 Å resolution: Kinetic and molecular dynamic correlates. *Biochemistry 41*, 2970−2981.
(57) Paz, A., Roth, E., Ashani, Y., Xu, Y., Shnyrov, V. L., Sussman, J. L., Silman, I., and Weiner, L. (2012) Structural and functional characterization of the interaction of the photosensitizing probe

methylene blue with *Torpedo californica* acetylcholinesterase. *Protein Sci. 21*, 1138−1152.
(58) Radic, Z., and Taylor, P. (2001) Interaction kinetics of reversible inhibitors and substrates with acetylcholinesterase and its fasciculin 2 complex. *J. Biol. Chem. 276*, 4622−4633.